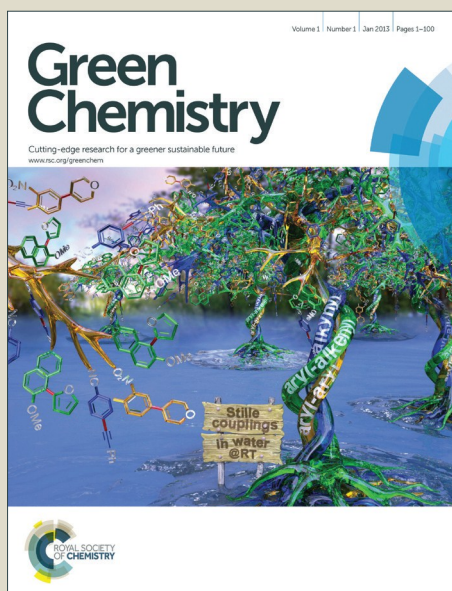


Green Chemistry

Accepted Manuscript



This article can be cited before page numbers have been issued, to do this please use: C. Zhang, J. Lu, X. Zhang, K. E. MacArthur, M. Heggen, H. Li and F. Wang, *Green Chem.*, 2016, DOI: 10.1039/C6GC01456A.



This is an *Accepted Manuscript*, which has been through the Royal Society of Chemistry peer review process and has been accepted for publication.

Accepted Manuscripts are published online shortly after acceptance, before technical editing, formatting and proof reading. Using this free service, authors can make their results available to the community, in citable form, before we publish the edited article. We will replace this *Accepted Manuscript* with the edited and formatted *Advance Article* as soon as it is available.

You can find more information about *Accepted Manuscripts* in the [Information for Authors](#).

Please note that technical editing may introduce minor changes to the text and/or graphics, which may alter content. The journal's standard [Terms & Conditions](#) and the [Ethical guidelines](#) still apply. In no event shall the Royal Society of Chemistry be held responsible for any errors or omissions in this *Accepted Manuscript* or any consequences arising from the use of any information it contains.



Green Chemistry

ARTICLE

Cleavage of lignin β -O-4 ether bond via dehydroxylation-hydrogenation strategy over a NiMo sulfide catalystChaofeng Zhang,^{a,b} Jianmin Lu,^a Xiaochen Zhang,^a Katherine MacArthur,^c Marc Heggen,^c Hongji Li^{a,b} and Feng Wang^{a*}Received 00th January 20xx,
Accepted 00th January 20xx

DOI: 10.1039/x0xx00000x

www.rsc.org/

Efficient cleavage of lignin β -O-4 ether bonds to produce aromatics is a challenging and attractive topic. Recently a growing number of studies reveal the initial oxidation of C_{α} HOH to C_{α} =O can decrease the β -O-4 bond dissociation energy (BDE) from 274.0 $\text{kJ}\cdot\text{mol}^{-1}$ to 227.8 $\text{kJ}\cdot\text{mol}^{-1}$, and thus the β -O-4 bond is more readily cleaved in the subsequent transfer hydrogenation, or acidolysis. Here we show that the first reaction step, except in the above-mentioned pre-oxidation methods, can be a C_{α} -OH bond dehydroxylation to form a radical intermediate on the acid-redox site of a NiMo sulfide catalyst. The formation of a C_{α} radical greatly decreases the C_{β} -OPH BDE from 274.0 $\text{kJ}\cdot\text{mol}^{-1}$ to 66.9 $\text{kJ}\cdot\text{mol}^{-1}$ thereby facilitating its cleavage to styrene, phenols and ethers with H_2 and alcohol solvent. This is supported by control experiments using several reaction intermediates as reactants, analysis of product generation and by radical trap with TEMPO (2,2,6,6-tetramethyl-1-piperidinyloxy) as well as by density functional theory (DFT) calculations. The dehydroxylation-hydrogenation reaction is conducted under non-oxidative condition, which is beneficial for stabilizing phenols products.

1. Introduction

Compared with other biomass targets, lignin has received a great amount of attention as it can potentially be used to prepare functionalized aromatic fine chemicals.¹ The key issue for the lignin transformation lies in the development of efficient catalysts and strategies to selectively cleave the stable and ubiquitous ether bonds, whilst leaving the aromatic benzene rings unconverted.²

The β -O-4 ether bond structure (Figure 1) accounts for 40–60% interunit linkage in lignin, and is the targeted bond to break during lignin degradation.^{1a} It also becomes the targeted activation bond in the hydrogenolysis,³ oxidation,⁴ acidolysis,⁵ alcoholysis,⁶ redox-neutral⁷ and tandem methods.⁸ Experimental studies combined with DFT calculations have shown that the substitutions at the C_{α} atom have a great effect on the bond dissociation energy (BDE) of the C_{β} -OPH bond and the activation of β -O-4 lignin linkage.^{7a-d, 8c, 9}

The C_{β} -OPH bond of β -O-4-Ketone has about 40 $\text{kJ}\cdot\text{mol}^{-1}$ lower dissociation energy than that of β -O-4-Alcohol, causing some studies to first convert C_{α} HOH to C_{α} =O (β -O-4-Ketone),

and then convert β -O-4-Ketone to other products.^{7a, 7b, 8c-e} In

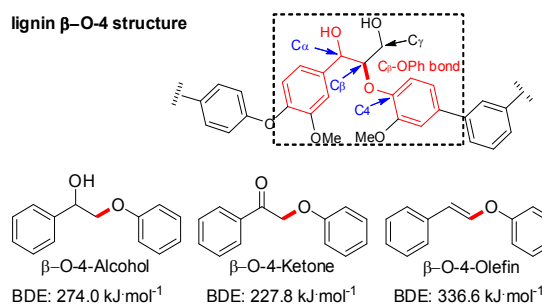


Figure 1. The structure of lignin β -O-4 linkage and transformation intermediates.

other reports, the β -O-4-Alcohol tends to dehydrate and generate a β -O-4-Olefin.^{7e, 7f, 10} However, the BDE of C_{β} -OPH ether bond in β -O-4-Olefin is about 61 $\text{kJ}\cdot\text{mol}^{-1}$ and 108 $\text{kJ}\cdot\text{mol}^{-1}$ higher than the C_{β} -OPH ether bonds in β -O-4-Alcohol and β -O-4-ketone (Figure 1). The different catalytic routes produce different intermediaries, which can cause variations in the C_{β} -OPH ether bond cleavage. While, the dominating factor for the C_{β} -OPH ether bond cleavage should not only contain the target bond BDE of the original substrate but also one of the activated intermediates' phase.^{5c, 7c, 7f} In an ideal route for cleavage of the β -O-4 bond, an activated intermediate is generated after a series of activation steps with low activation energy, whose target bond has a lower energy and easily breaks in the subsequent transformations. The unique properties of catalysts should play dominative roles in the activation route control.

^a State Key Laboratory of Catalysis, Dalian National Laboratory for Clean Energy, Dalian Institute of Chemical Physics, Chinese Academy of Sciences, Dalian 116023 (China)

^b University of Chinese Academy of Sciences, Beijing 100049 (China)

^c Ernst Ruska Centre for Microscopy and Spectroscopy with Electrons and Peter Grünberg Institute, Forschungszentrum Juelich GmbH, Juelich 52425 (Germany)

* Corresponding author. E-mail: wangfeng@dicp.ac.cn

Electronic Supplementary Information (ESI) available: Lignin β -O-4 model compounds synthesis, catalysts preparation, ether bonds BDE, control experiments. See DOI: 10.1039/x0xx00000x

Although heterogeneous catalysts have been widely used in the catalytic hydrogenation and alcoholysis lignin processes,¹¹ research pays more attention to the conversion promotion than the mechanism of ether bond cleavage,^{2b, 3k, 7c} which usually references to the concept of homogeneous catalysis.^{7a, 7b, 7d, 7e, 12} In order to further optimize the lignin conversion over heterogeneous catalysts, new understanding about the mechanism of ether bonds cleavage is necessary, which is conducive to the exploration of new strategies and catalysts.

In this work, we employed as-synthesized NiMo and other MMO sulfide catalysts (M=Mn, Fe, Co) in the hydrogenation of lignin β -O-4 model compounds.^{11k, 11l, 13} After optimization of the reaction condition, the NiMo sulfide catalyst achieved preferential cleavage of ether bonds and preserved the aromatic rings. Conversions of different β -O-4 model compounds showed that the efficiency of C_{β} -OPh bond cleavage was not controlled by BDE value of the substrate C_{β} -OPh bond. For instance, the β -O-4 lignin model compound with C_{α} HOH transformed more easily than the one with C_{α} =O over NiMo sulfide catalyst. This differs from previous reports.^{2b, 8c, 8d} Based on the control experiments, product generation analysis and DFT calculation results, we found that the substrate activation routes play a crucial role in the ether bond cleavage efficiency and products distribution.

In contrast to the previously reported strategies beginning with dehydrogenation,^{8c-e} we propose a new dehydroxylation-hydrogenation strategy to achieve preferential cleavage of the ether bond in β -O-4-Alcohol. The method begins with a dehydroxylation reaction of the C_{α} -OH in β -O-4-Alcohol which generates a possible intermediate $\text{PhCH}^{\delta+}\text{CH}_2\text{OPh}$. This process contains a carbocation ($\text{PhCH}^{\delta+}\text{CH}_2\text{OPh}$) generation and its reduction. Then the cleavage of C_{β} -OPh ether bond in the radical intermediate occurs. DFT calculation results show that this process can decrease the BDE value of C_{β} -OPh bond in the $\text{PhCH}\cdot\text{CH}_2\text{OPh}$ intermediate from 274.0 $\text{kJ}\cdot\text{mol}^{-1}$ to 66.9 $\text{kJ}\cdot\text{mol}^{-1}$.

2. Results and discussion

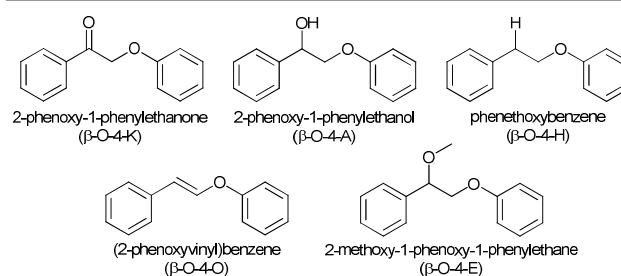
2.1 Cleavage of β -O-4 ether linkages over the NiMo sulfide catalyst

The β -O-4 ether bond is the primary targeted bond to break during lignin degradation.^{1a} In this work (Scheme 1), we choose 2-phenoxy-1-phenylethanone (β -O-4-K), 2-phenoxy-1-phenylethanol (β -O-4-A), (2-phenoxyethyl)benzene (β -O-4-H), (2-phenoxyvinyl)benzene (β -O-4-O), (1-methoxy-2-phenoxyethyl)benzene (β -O-4-E) and their analogues as β -O-4 linkage model compounds and the possible intermediates.

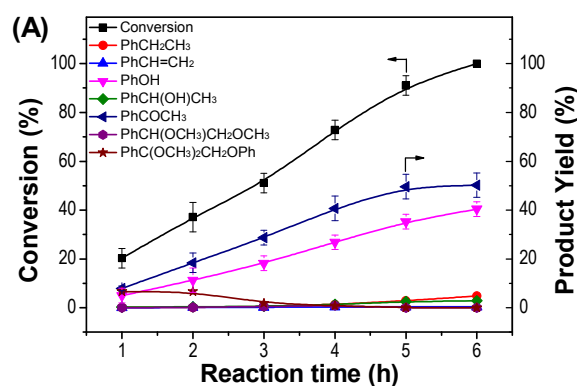
In the hydrogenation of β -O-4-K (Figure 2A), the NiMo sulfide catalyst preferentially catalyzed the cleavage of C_{β} -OPh bond over the hydrogenation of $C=O$ bond. The main products were acetophenone and phenol, and no aromatic rings were hydrogenated. Small amounts of ethylbenzene and (1-methoxyethyl)benzene generated in the products as the reaction proceeded. The reaction offered 99% conversion of β -O-4-K in 6 hours.

In the hydrogenation of β -O-4-A (Figure 2B), the NiMo sulfide catalyst selectively catalyzed the cleavage of the C_{β} -OPh bond, and no products with aromatic ring hydrogenated were detected. The main products with C_{β} -OPh bond cleavage during the earlier stage of reaction (<0.5 hour) were styrene, phenol, (1-methoxyethyl)benzene and (2,2-dimethoxyethyl)benzene. Although a 69% conversion was obtained after 1 hour at 180 °C, the main product (35%) of β -O-4-A transformation was β -O-4-E without ether bond cleavage. Compared with β -O-4-K conversion with C_{β} -OPh bond cleavage (14%), the β -O-4-A conversion with C_{β} -OPh bond cleavage (33%) was higher at the same reaction condition in 1 hour.

To further confirm the β -O-4-A with C_{α} H-OH structure was more easily transformed than the β -O-4-K with C_{α} =O structure over the NiMo sulfide catalyst, we carried out the control experiment with β -O-4 model compounds with C_{α} H-OH and C_{α} =O group in one reactor. In the competitive conversion of β -O-4-A-OCH₃ and β -O-4-K (Scheme 2A), the products of conversion of β -O-4-K were small amount of PhC_2H_5 , PhOH and PhCOCH_3 (Figure S11). The quantitative relationships among the converted β -O-4-A-OCH₃ and β -O-4-K with C_{β} -OPh bond cleavage, PhOH and PhCOCH_3 was shown in Scheme 2A. The



Scheme 1. The β -O-4 linkage model compounds.



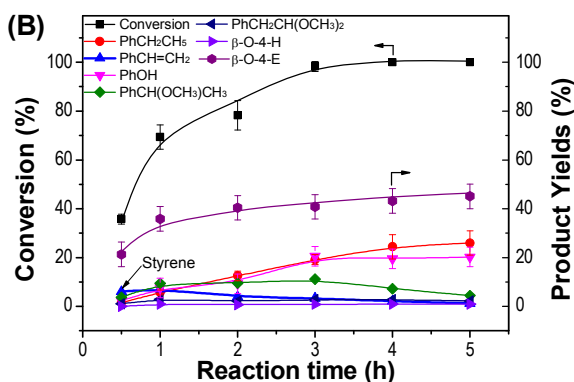
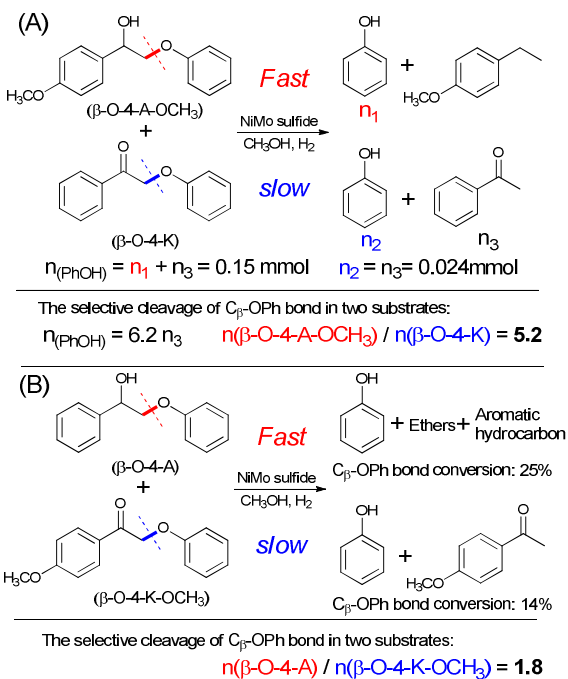


Figure 2. The conversion of β -O-4-K (A) and β -O-4-A (B) over the NiMo sulfide catalyst. Reaction condition: substrate 0.2 mmol, catalyst 20 mg, methanol 2.0 mL, H_2 1.0 MPa, 180 °C.



Scheme 2. The competitive conversion of β -O-4 model compounds with C_{α} H-OH and C_{α} =O group in one reactor. Reaction condition: each model compound 0.2 mmol, NiMo sulfide 20 mg, methanol 2.0 mL, H_2 1.0 MPa, 180 °C, 1 h. The $n(\text{substrate})$ stands for the amounts of converted substrate with C_{β} -OPh bond cleavage.

amounts of PhOH was 6.2 times of PhCOCH₃, which showed that the conversion of β -O-4-A-OCH₃ with C_{β} -OPh bond cleavage to PhOH was 5.2 times of β -O-4-K. Furthermore, the cleavage of C_{β} -OPh bond in the competitive conversion of β -O-4-A-OCH₃ and β -O-4-K under Ar condition was not obvious (Figure S12). In the competitive reaction of β -O-4-A and β -O-4-K-OCH₃ (Scheme 2B), the C_{β} -OPh bond conversion difference reduced to 1.8 times. These results showed that NiMo sulfide

preferred to catalyze the hydrogenative cleavage of C_{β} -OPh bond connecting with a C_{α} H-OH structure.

The high rate of conversion and aromatic products with ether bond cleavage showed that the NiMo sulfide was an efficient catalyst for the selective conversion of β -O-4 model compounds. The generation of β -O-4-E will be discussed in the following section about the possible reaction route (Scheme 6). Approaches for decreasing the β -O-4-E were also explored (Figure S15). Furthermore, when TEMPO as a shielding reagent of radical route was added in the hydrogenation of β -O-4-A (Scheme S3), conversion was not obvious (<1%). When reaction carried out under Ar condition (Scheme S4), only 1% C_{β} -OPh bond in β -O-4-A cleaved. These results indicated the reaction probably occurred through a radical route,¹⁴ and the acid sites (Figure S10) of the NiMo sulfide alone could not catalyze the transformation of β -O-4-A via dehydration-hydrolysis route.^{5a, 5c}

2.2 The effect of the functional group at the C_{α} atom

In the hydrogenation of lignin model compounds, the reaction route plays a crucial role in the bonds selective cleavage and products distribution, which is controlled by substrate structure and catalyst properties.^{2b, 7b, 7c, 8c, 8d, 14}

The functional group attached to the C_{α} atom has a remarkable effect on the BDE value of C_{β} -OPh ether bond in β -O-4 model compounds (Table S1). The alkyl-OPh bond energy of β -O-4-A is 274.0 kJ·mol⁻¹, 46.2 kJ·mol⁻¹ higher than the one in the β -O-4-K. It is 275.3 kJ·mol⁻¹ for the alkyl-OPh bond in the β -O-4-H. Additionally, the BDE of the alkenyl-OPh ether bond in the β -O-4-O increases to 336.6 kJ·mol⁻¹ which is nearly 110 kJ·mol⁻¹ higher than the alkyl-OPh bond in the β -O-4-K. Based on the ether bond BDE energy order (β -O-4-K < β -O-4-A \approx β -O-4-H < β -O-4-O), the two-step method is usually employed in the conversion of the β -O-4 lignin model compounds, which contains a preoxidizing step to oxidize C_{α} H-OH to C_{α} =O before a subsequent transfer hydrogenation or acidolysis.^{8c-e}

The conversion of lignin β -O-4 model compounds over the NiMo sulfide catalyst is not consistent with the BDE energy order (Table 1). Even though the BDE of C_{β} -OPh ether bond in β -O-4-K is 46.2 kJ·mol⁻¹ lower than the one in β -O-4-A, the conversion of C_{β} -OPh bond in β -O-4-A (33%) is almost two and a half times of the one of C_{β} -OPh bond in β -O-4-K (14%). No ether bonds cleave during the conversion of β -O-4-H, despite it having the approximate C_{β} -OPh bond BDE as β -O-4-A. The β -O-4-O has a highest ether bond BDE (336.3 kJ·mol⁻¹) and it offers a 37% conversion with ether bond cleavage. These results show the effect of substrate structure on the conversion of ether bond cleavage in lignin β -O-4 model compounds, and the dominative factor of the conversion is not the BDE value of target ether bond in the original substrate.

Table 1. The difference of the β -O-4 lignin model compounds conversion over the NiMo sulfide catalyst.^a

Entry	Substrate	BDE (kJ·mol ⁻¹)	Conv. (%)	Products distribution (%) ^b															
1		274.0	33%	62	14	0	0	0	0	0	0	0	0	0	0	0	0	0	0
2		275.3	14%	14	0	0	0	0	0	0	0	0	0	0	0	0	0	0	0
3		275.3	0%	0	0	0	0	0	0	0	0	0	0	0	0	0	0	0	0
4		336.6	37%	0	0	0	0	0	0	0	0	0	0	0	0	0	0	0	0

1		274.0	69 (33) ^c	8	10	11	13	0	4	1	52	0
2		227.8	20 (14) ^c	<1	<1	25	1	40	0	0	<1	33
3		275.3	No (0) ^c	0	0	0	0	0	0	0	0	0
4		336.6	37 (37) ^c	8	10	20	4	0	58	0	0	0

^a Reaction conditions: substrate 0.2 mmol, NiMo sulfide catalyst 20 mg, methanol 2.0 mL, H₂ 1.0 MPa, 180 °C, 1 h. ^b The distribution ratio of each product was calculated basing on the total molar amount of GC products with and without C_β-OPh ether bond cleavage. ^c C_β-OPh ether bond cleavage conversion.

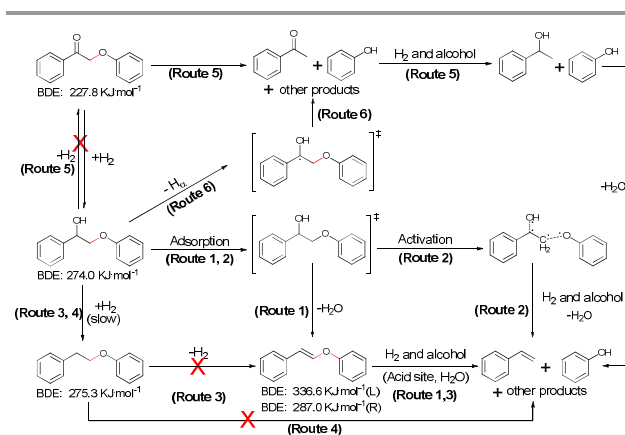
2.3 The possible routes for the β-O-4-A conversion over the NiMo sulfide catalyst based on the styrene generation

One reason for the discrepancy between C_β-OPh bonds conversions and their BDE value could be that β-O-4-A has undergone a conversion to an active intermediate,^{7c} whose target ether bond has a lower energy that makes the conversion process more competitive.

We detected 7% yield of styrene in products (arrowed in Figure 2B), which was seldom detected in earlier studies.^{7e, 11b}

The styrene generation in the β-O-4-A conversion implies a different reaction route. Regarding styrene as the target product (Scheme S1), we propose the possible routes of β-O-4-A transformation (Scheme 3). (1) β-O-4-A loses a H₂O and generates β-O-4-O,¹⁵ then the β-O-4-O transforms to styrene and phenol in the subsequent direct hydrogenation, or the styrene generation is a acidolysis-hydrogenation-dehydration process with a PhCH₂CHO intermediate.^{5a-c} (2) Cleavage of C_β-OPh bond in β-O-4-A occurs, and then the intermediate (PhCH(OH)CH₂·) transform to styrene directly after losing a hydroxy radical at C_α or via a PhCH(OH)CH₃ intermediate. Alternatively, the β-O-4-A loses a hydroxyl group at C_α, then the intermediate (PhCH·CH₂OPh) transforms to the styrene, phenol and other products after the cleavage of C_β-OPh ether bond. (3) β-O-4-A hydrogenolysis generates a β-O-4-H, then the subtraction of two hydrogen atoms from β-O-4-H results in a β-O-4-O, which is subsequently converted into styrene and phenol. (4) The C_β-OPh ether bond in β-O-4-H cleaves, and then the generated radical intermediate (PhCH₂CH₂·) loses an H· radical to generate the styrene.^{11b} (5) β-O-4-A transforms to β-O-4-K via a dehydrogenation process,^{11h} then the hydrogenated product acetophenone transforms to the styrene. (6) C_β-OPh bond of the dehydrogenation intermediate (PhC(OH)CH₂OPh or PhCH(OH)CH₂OPh) cleaves, and the generated species transforms to PhCOCH₃ or be hydrogenated to PhCH(OH)CH₃, then PhCH(OH)CH₃ transforms to styrene.

The ratio of C_β-OPh bond cleavage in β-O-4-A conversion is higher than β-O-4-K and β-O-4-H (Table 1, Entries 1-3). No acetophenone as the representative product of the β-O-4-K or PhC(OH)CH₂OPh hydrogenolysis is generated in β-O-4-A conversion, which indicates the main β-O-4-A conversion process does not contain the dehydrogenation step at C_α atom.



Scheme 3. The routes for styrene generation in β-O-4-A conversion over the NiMo sulfide catalyst.

Comparing with the active hydrogen of C_α-H_α and C_α-H-OH_β in β-O-4-A (PhC_αH(OH)C_βH₂OPh), the hydrogen of C_β-H_β is a relative inert one. During the previous reports about the first step of β-O-4-A activation, the target bond is C_α-H-OH_β^{4d, 7b, 7d, 7f} or C_α-H_α^{7c, 7e} not the C_β-H_β bond. Furthermore, the β-O-4-H conversion over NiMo sulfide catalyst is not obvious (Table 1, Entry 3), and there is only 1% β-O-4-H in the β-O-4-A conversion products (Table 1, Entry 1). The hydrogenolysis of the hydroxyl group at C_α atom of β-O-4-A to β-O-4-H over the NiMo sulfide catalyst occurs slowly. These results indicate that Routes 3-6 are not the main route for the β-O-4-A conversion over the NiMo sulfide catalyst.

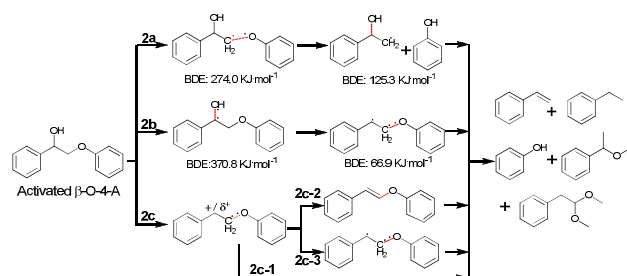
In Route 1, the activated β-O-4-A loses a H₂O and generates a β-O-4-O. When β-O-4-O was used as the substrate (Table 1, Entry 4), a 37% conversion was obtained in 1 hour at 180 °C and the main products generated with C_β-OPh ether bond cleavage, which presented a potential application method (dehydration-hydrogenation).^{7e, 7f, 15} When the β-O-4-A was used as the substrate (Table 1, Entry 1), an approximate conversion with ether bond cleavage (33%) was obtained. However, the main ether product of β-O-4-O conversion was (2,2-dimethoxyethyl)benzene, which was only a minor ether product in the β-O-4-A conversion (Table 1, Entries 1 and 4). The main ether product, also the byproduct without ether bond cleavage, β-O-4-E in the β-O-4-A conversion was not detected in the β-O-4-O conversion. Furthermore, the generation of β-O-4-O from β-O-4-A via a dehydration process was not obvious under Ar condition (Scheme S4). These differences indicated that Route 1 was not the main route of β-O-4-A conversion over the NiMo sulfide catalyst.

The BDE value of C_{β} -OPh ether bond in β -O-4-O was $336.3 \text{ kJ}\cdot\text{mol}^{-1}$, which was higher than C_{β} -OPh bonds in β -O-4-A, β -O-4-H, β -O-4-K and the C_{β} -OPh bond in β -O-4-O (Scheme 3). However, it did give the highest conversion. This anomaly raises another question: whether the C_{β} -OPh bond in the β -O-4-O cleaved directly or the β -O-4-O conversion occurred via an intermediate with lower BDE ether bond. This question is discussed in the following part about ether generation from β -O-4-O (Scheme 6 and Figure 3).

2.4 The Route 2 for β -O-4-A conversion

In route 2, based on the cleavage order of the C_{α} -OH and C_{β} -OPh bonds, there are three plausible routes for the β -O-4-A conversion to styrene (Scheme 4): (2a) C_{β} -OPh ether bond in β -O-4-A cleaves, and then the intermediate ($\text{PhCH}(\text{OH})\text{CH}_2\cdot$) transform to styrene. (2b) β -O-4-A loses a hydroxy radical and generates a radical intermediate ($\text{PhCH}\cdot\text{CH}_2\text{OPh}$), after which C_{β} -OPh ether bond cleaves and generates a styrene. (2c) β -O-4-A loses a hydroxy group and generates a carbocation intermediate ($\text{PhCH}^+\text{CH}_2\text{OPh}$ or $\text{PhCH}^{\delta+}\text{CH}_2\text{OPh}$),^{3k, 5a, 5b} which then transforms to the styrene after some activation.

As shown in Table 1, the C_{β} -OPh bond BDEs in β -O-4-A and β -O-4-H are approximate. However, when an H atom replaces the OH group at C_{α} , the β -O-4-H shows no conversion, but β -O-4-A conversion with ether bond cleavage is about 33%. The obvious difference shows the effect of C_{α} -OH group on the C_{β} -OPh bond cleavage. In the heterogeneous catalysis process, substrate adsorption is the origin of the substrate activation.



Scheme 4. The route 2 for β -O-4-A conversion with different cleavage order of C_{β} -OPh ether bond and C_{α} -OH bond.

The removal of polar hydroxy group can affect the absorption of β -O-4-H onto the NiMo sulfide catalyst. However, taking into account the good conversion of β -O-4-O, which also contains no polar group at the C_{α} atom, we can see that the promotion of absorption by the polar group at C_{α} atom is limited in the cleavage of C_{β} -OPh bond. The effect of the C_{α} -OH can be attributed to how critical the C_{α} -OH transformation is for C_{β} -OPh bond conversion^{11h} over NiMo sulfide catalyst.

In route 2a, the C_{β} -OPh bond breaks directly without C_{α} -OH transformation. This is similar to the conversion of β -O-4-K with acetophenone and phenol as the main products. While, β -O-4-A with higher ether bond BDE transforms more easily than β -O-4-K, it indicates that Route 2a may not be an efficient route for the β -O-4-A conversion over the NiMo sulfide catalyst. In addition, there is no catalysis system achieving β -O-4-A conversion via the direct cleavage of C_{β} -OPh bond, and the

activation of the $C_{\alpha}\text{HO-H}_O$ ^{4d, 7b, 7d, 7f} or $C_{\alpha}\text{-H}_\alpha$ ^{7c, 7e} usually occurs firstly before the cleavage of C_{β} -OPh bond. Taking into account that β -O-4-A with $C_{\alpha}\text{H-OH}$ structure is more easily transformed than β -O-4-K with $C_{\alpha}=\text{O}$ structure over the NiMo sulfide catalyst, new reaction route should exist. As discussed before, the C_{α} -OH transformation is critical for cleavage of C_{β} -OPh bond, we should discuss the potential routes with C_{α} -OH bond cleavage.

Routes 2b and 2c both begin with C_{α} -OH bond cleavage, and the cleavage occurs by homolysis in Route 2b and heterolysis in Route 2c. For the C_{α} -OH homolysis in Route 2b, the BDE of the C_{α} -OH is $370.8 \text{ kJ}\cdot\text{mol}^{-1}$, which is $96.8 \text{ kJ}\cdot\text{mol}^{-1}$ higher than the C_{β} -OPh bond in the same molecule. This makes Route 2b more complex than Route 2a and it has a C_{α} -OH bond with a higher BDE to cleave.

In route 2c, β -O-4-A loses a hydroxy group and generates a carbocation ($\text{PhCH}^+\text{CH}_2\text{OPh}$ or $\text{PhCH}^{\delta+}\text{CH}_2\text{OPh}$) intermediate, which involves acid-catalysed benzyl hydroxy heterolysis dehydroxylation and can occur easily at acid sites.^{3k, 5a, 5b} Based on the NH_3 -TPD result (Figure S10), the NiMo sulfide catalyst contains weak and medium strong acid sites, and the NH_3 absorption capacity is $90.2 \mu\text{mol}\cdot\text{g}^{-1}$. Different from benzyl hydroxy heterolysis with strong protonic acid to generate a free carbocation ($\text{PhCH}^+\text{CH}_2\text{OPh}$),^{5a, 5b} weak and medium strong acid sites of NiMo sulfide trend to achieve the heterolysis dehydroxylation via a adsorbed intermediate of $\text{C}^{\delta+}\cdots\delta^-\text{OH-Acid site}$.^{3k} For the heterolysis dehydroxylation of β -O-4-A over the acid sites of NiMo sulfide, trace amount of β -O-4-O as an acid-catalyzed product is detected during β -O-4-A conversion under Ar condition (Scheme S4). Styrene is detected in 1-phenethyl alcohol conversion (Figure S13B). Additionally, the addition of KOH can decrease the β -O-4-A conversion with ether bond cleavage to only 2% under H_2 condition (Scheme S4).

In later steps of Route 2c, the ether bond cleavage of adsorbed $\text{PhCH}^{\delta+}\text{CH}_2\text{OPh}$ can occur directly and generate a $\text{PhCH}^{\delta+}\text{CH}_2\cdot$ (Route 2c-1), which has two unstable structures suggesting its generation should be difficult. In other transformations, the adsorbed $\text{PhCH}^{\delta+}\text{CH}_2\text{OPh}$ can lose an H^+ at C_{β} to β -O-4-O (Routes 2c-2 or 1).^{5a} However, as discussed earlier, even though the dehydration-hydrogenation route (Route 1) is an efficient route, it is not the main route here. Furthermore, if conditions permit, the adsorbed $\text{PhCH}^{\delta+}\text{CH}_2\text{OPh}$ can transform to an adsorbed radical intermediate ($\text{PhCH}\cdot\text{CH}_2\text{OPh}$) after obtaining an electron from the catalyst redox cycle (Route 2c-3). The BDE of C_{β} -OPh ether bond in $\text{PhCH}\cdot\text{CH}_2\text{OPh}$ can be reduced to only $66.9 \text{ kJ}\cdot\text{mol}^{-1}$ (Table S1).

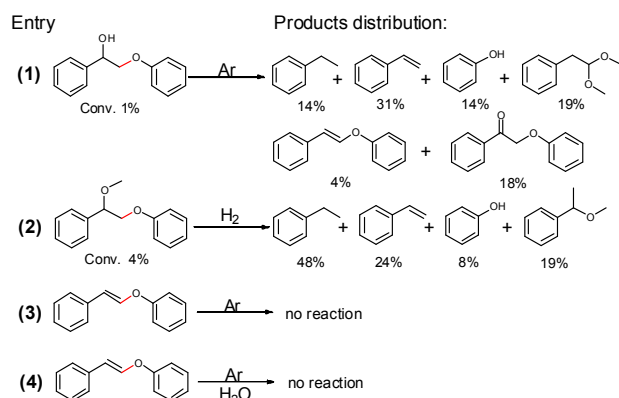
Referring to the enthalpy change of heterolysis dehydroxylation ($\text{PhCH}(\text{OH})\text{CH}_2\text{OPh} + \text{H}^+ \rightarrow \text{PhCH}^+\text{CH}_2\text{OPh} + \text{H}_2\text{O}$; $\Delta\text{H} = 49.4 \text{ kJ}\cdot\text{mol}^{-1}$)^{5a} and direct dehydroxylation ($\text{PhCH}(\text{OH})\text{CH}_2\text{OPh} \rightarrow \text{PhCH}\cdot\text{CH}_2\text{OPh} + \text{HO}\cdot$; $\Delta\text{H} = 370 \text{ kJ}\cdot\text{mol}^{-1}$), Route 2c-3 containing carbocation generation and reduction to $\text{PhCH}\cdot\text{CH}_2\text{OPh}$ could be regarded as the optimization of Route 2b (Scheme S2). This is especially feasible when considering the fact that adsorbed $\text{PhCH}\cdot\text{CH}_2\text{OPh}$ should have a lower energy than its gas phase. This provides that Route 2c-3 has

the potential to promote the cleavage of C_β-OPh bond.

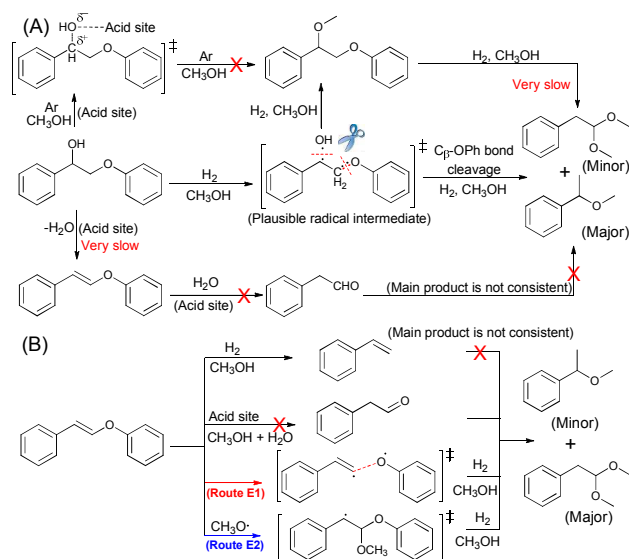
2.5 The analysis of ether compounds generation for understanding β-O-4-A conversion

Besides the analysis of styrene generation, analysis of ethers generation is also important to improve our understanding about the main reaction route. As shown in Scheme 5, for the ether compound generation from alcohols, there are two mechanisms, with either a carbocation or radical intermediate.

In order to confirm the generation route of ether compounds, various control experiments were carried out. Firstly, we checked the β-O-4-A conversion under the Ar atmosphere, where only 1% conversion was obtained (Scheme



Scheme 5. The conversion of the β-O-4 model compounds. Reaction conditions: substrate 0.2 mmol, catalyst 20 mg, methanol 2.0 mL, 1.0 MPa H₂ or 1.0 MPa Ar, 180 °C, 1 h. In the reaction under Ar condition, the catalyst is pre-treated at 180 °C for 1 h in the methanol under 1.0 MPa H₂. The amount of water added in Entry 4 is 200 μL.



Scheme 6. The routes of ether products generation in the conversion of β-O-4-A (A) or β-O-4-O (B) over the NiMo sulfide catalyst.

5, Entry 1). The change of NH₃ absorption capacity for the NiMo sulfide catalyst is inconspicuous after its treatment in the methanol under H₂ (Figure S10), which indicates that the weak and medium strong acid sites of NiMo sulfide show low

activity alone. The β-O-4-A conversion over NiMo sulfide is not a simple acid-catalysed process to PhCH₂CHO with a free carbocation (PhCH⁺CH₂OPh) intermediate.^{5a-c} Given the result that the main product (Entry 1), also ether product of PhCH₂CHO conversion (Scheme S7), is PhCH₂CH(OCH₃)₂, which is different from β-O-4-A conversion with PhCH(OCH₃)CH₃ as the main ether product of C_β-OPh cleavage. The β-O-4-A conversion over NiMo sulfide is not an acidolysis-etherification or acidolysis-hydrogenation process, which produce ether compounds and PhCH=CH₂ with PhCH₂CHO as the key intermediate (Scheme 6A).^{5b}

Furthermore, the different conversions of β-O-4-A under H₂ (Table 1, Entry 1) and Ar (Scheme 5, Entry 1) demonstrates how critical H₂ is in β-O-4-A conversion and ether generation. There is no β-O-4-E but small amount of other ethers in the β-O-4-A conversion under Ar, which indicates that the generation of the ether compounds, especially for the β-O-4-E, probably occurs via a radical intermediate under H₂ over the NiMo sulfide catalyst (Scheme 6A). For the β-O-4-E generation, its precursor should be the adsorbed PhCH·CH₂OPh. Furthermore, β-O-4-E conversion is only 4% at 1 h (Scheme 5, Entry 2), which is much lower than the β-O-4-A conversion (Table 1, Entry 1). The most ether products with C_β-OPh bond cleavage in β-O-4-A conversion should not generate from β-O-4-E but from the plausible radical intermediate (Scheme 6A).

In order to further confirm the main route of β-O-4-A conversion and the cleavage order of C_α-OH and C_β-OPh bonds during the ether products generation (Scheme 6A), the first analysis about the β-O-4-O conversion without C_α-OH might be conducive to understand the β-O-4-A conversion (Scheme 6B).

There is a high percentage of PhCH₂CH(OCH₃)₂ in β-O-4-O conversion products (Table 1, Entry 4). For its generation, when styrene was used as the substrate (Scheme S6), there were only PhCH₂CH₃, PhCH(OCH₃)CH₃ and some condensation compounds in the products, but no PhCH₂CH(OCH₃)₂. So, the PhCH₂CH(OCH₃)₂ is not generated from styrene. In addition, no β-O-4-O conversion is detected under Ar condition (Scheme 5, Entry 3, 4). This result indicates the acid sites on the NiMo sulfide catalyst alone cannot promote the β-O-4-O transformation to PhCH₂CHO, which is a typical acid-catalyzed product and the precursor of PhCH₂CH(OCH₃)₂ even under Ar condition (Scheme S7).^{5a, 5b} The ether compounds should generate via a radical route over the NiMo sulfide.

Regarding PhCH₂CH(OCH₃)₂ as the target product in the β-O-4-O transformation, based on the order of C_β-OPh bond cleavage and C_β-OCH₃ bond generation, two radical routes are proposed (Scheme 6B). (Route E1) C_β-OPh ether bond in β-O-4-O cleaves directly and generates a PhCH=CH· radical, which then reacts with methanol or methoxyl radical to the ethers under H₂. (Route E2) One methoxyl radical should have connected with the activated β-O-4-O and generates a radical intermediate (PhCH·CH(OCH₃)OPh) before the cleavage of C_β-OPh ether bond, then the generated PhCH=CH(OCH₃) reacts with methanol or methoxyl radical to PhCH₂CH(OCH₃)₂.

DFT calculation is employed to compare these two radical routes. The direct cleavage of C_β-OPh bond in β-O-4-O has a 336.6 kJ·mol⁻¹ BDE in Route E1. When the C_β of β-O-4-O

combines with a methoxyl radical in Route E2, the C_{β} -OPh bond BDE in PhCH·CH(OCH₃)OPh decreases obviously to 41.2 kJ·mol⁻¹ (Table S1), which is also much lower than the C_{β} O-Ph bond (199.6 kJ·mol⁻¹) in the same PhCH·CH(OCH₃)OPh intermediate. As shown in Figure 3A, the enthalpy change of direct cleavage of C_{β} -OPh bond in β -O-4-O is 336.6 kJ·mol⁻¹, and the enthalpy change of PhCH·CH(OCH₃)OPh generation from β -O-4-O and CH₃O· is -133 kJ·mol⁻¹. The obvious difference between two reaction enthalpy changes shows that the preponderant reaction route is not Route E1 but Route E2 (Scheme 6B). The much lower BDE of the C_{β} -OPh ether bond in PhCH·CH(OCH₃)OPh intermediate can also explain the fact that

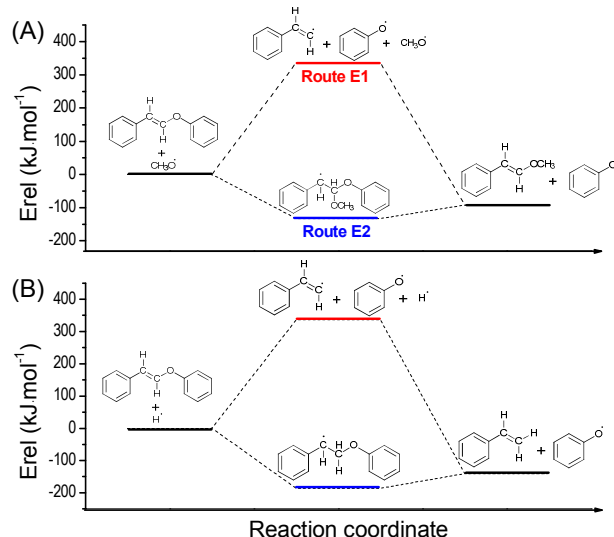


Figure 3. Enthalpy profile of the β -O-4-O transformation in the gas phase.

β -O-4-O with highest C_{β} -OPh ether bond BDE can be selectively and efficiently transformed.

Furthermore, styrene also generates in the β -O-4-O conversion. Referencing to the PhCH₂CH(OCH₃)₂ generation via Route E2, when an H· radical replaces the CH₃O· radical to attack the C_{β} atom (Figure 3B), the possible intermediate PhCH·CH₂OPh has a much lower C_{β} -OPh bond BDE (66.9 kJ·mol⁻¹) than β -O-4-O (336.6 kJ·mol⁻¹) or β -O-4-A (274.0 kJ·mol⁻¹). And the enthalpy change of PhCH·CH(OCH₃)OPh generation from β -O-4-O and H· is -186 kJ·mol⁻¹, which is obviously lower than the direct cleavage of C_{β} -OPh bond in β -O-4-O. These results suggest that the PhCH·CH₂OPh could be a key intermediate in the β -O-4-O conversion to styrene.

During β -O-4-A transformation, as discussed above, β -O-4-E generates via the PhCH·CH₂OPh radical intermediate, and other ether products with C_{β} -OPh bond cleavage generates from the plausible radical intermediate, whose structure correlates with the cleavage order of C_{α} -OH and C_{β} -OPh bonds (Scheme 6A). The obvious change of ether bond BDE among β -O-4-A, β -O-4-O and PhCH·CH₂OPh suggests the possibility of PhCH·CH₂OPh as the intermediate in the β -O-4-A transformation to ether compounds and styrene over NiMo catalyst. The NiMo sulfide catalyst prefers to catalyze the

cleavage of C_{α} -OH bond before the subsequent cleavage of C_{β} -OPh bond.

2.6 The potential Route 2c-3 for β -O-4-A transformation over NiMo sulfide catalyst

Based on the analysis of styrene and ethers generation, Route 2c-3 is the potential main route of β -O-4-A conversion over the NiMo sulfide catalyst (Figure 4). (1) The adsorbed β -O-4-A firstly loses a hydroxy group and generates a carbocation intermediate (PhCH ^{δ^+} CH₂OPh) at the acid site of the NiMo sulfide catalyst. (2) The PhCH ^{δ^+} CH₂OPh then transforms to the free radical intermediate (PhCH·CH₂OPh) by obtaining an electron from the catalyst redox cycle. (3) Because of the lower BDE of the C_{β} -OPh ether bond in the PhCH·CH₂OPh intermediate, the C_{β} -OPh bond cleaves and the generated radical species reacts with activated H₂ or methanol to various arenes, phenol and ether products. (4) As a side reaction, the PhCH·CH₂OPh can also react with activated methanol and generates a β -O-4-E without C_{β} -OPh bond cleavage.

2.7 The promotion effects for the β -O-4-A conversion

In the C_{β} -OPh ether bond selective cleavage, besides the influence factors of the bonds BDE and adjacent substituent groups' structure, the NiMo sulfide heterogeneous catalyst characterizations should also play a crucial role in substrate activation and catalytic reaction route determination.

Based on the potential reaction mechanism (Figure 4), there is a cooperation between the acid-redox site and hydrogenation site. This cooperation causes the NiMo sulfide catalyst to prefer C_{α} -OH the mechanism that generates a PhCH·CH₂OPh intermediate for the following C_{β} -OPh bond cleavage over catalysing β -O-4-A hydrogenolysis to the inert β -O-4-H.

As shown in Figure 5A, there are MoS₂ phase and NiS phase peaks existence in the XRD pattern of the NiMo sulfide catalyst. Besides these peaks, there are peaks attributed to Ni_{0.7}Mo₃S₄,

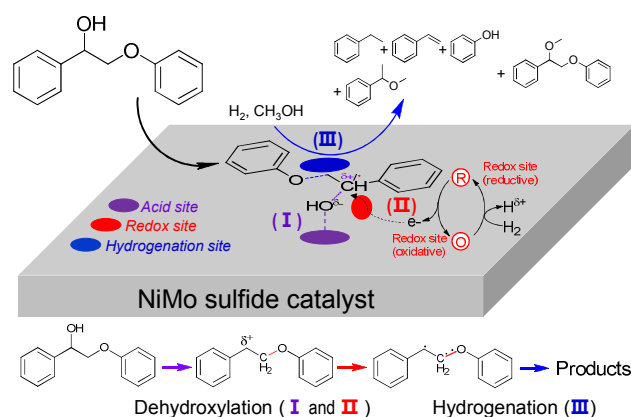


Figure 4. The potential Route 2c-3 for β -O-4-A conversion over the NiMo sulfide catalyst.

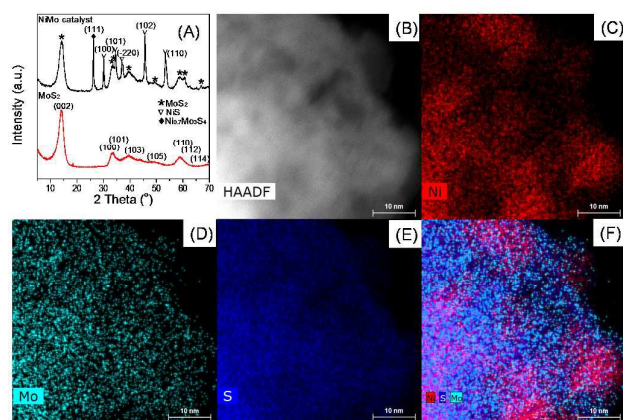


Figure 5. The x-ray diffraction pattern (A), annular dark-field scanning transmission electron microscopy image (B) of the NiMo sulphide catalysts. (C-E) show the element maps of Ni, Mo and S from energy dispersive x-ray analysis with the compound image of all three elements in (F). The bar inserting the image stands for 10 nm.

which is one of the Ni doped heterometallic cubane-type Mo clusters. Elements mapping results (Figure 5C-F) shows the Mo and S are uniformly distributed, and the Ni species appears aggregation to about 10 nm in some zones, which is corresponding to the NiS phase and Ni_{0.7}Mo₃S₄ phase in the XRD pattern of the NiMo sulfide catalyst. Based on the NH₃-TPD result (Figure S10), the NiMo sulfide catalyst contains weak and medium strong acid sites, and its NH₃ absorption capacity is 90.2 μmol·g⁻¹. For the acid sites, they could be attributed to the coordinative unsaturated Mo or Ni ion centres.¹⁶

When NiS was used as the catalyst, the cleavage of C_β-OPh bond was not obvious (Figure 6A), and β-O-4-A mainly reacted with the alcohol solvent to the etherification product of β-O-4-E. During the β-O-4-A transformation catalyzed by MoS₂ (Figure 6B), besides the etherification product of β-O-4-E and products with C_β-OPh bond cleavage, lots of β-O-4-H generated in this process. Although the β-O-4-H was a by-product, its generation suggested the existence of the intermediate PhCH·CH₂OPh, which preferred to react with the active H· to β-O-4-H rather than cleave the C_β-OPh bond over the MoS₂ catalyst. Compared with MoS₂ catalyst performance, Ni species introducing in the

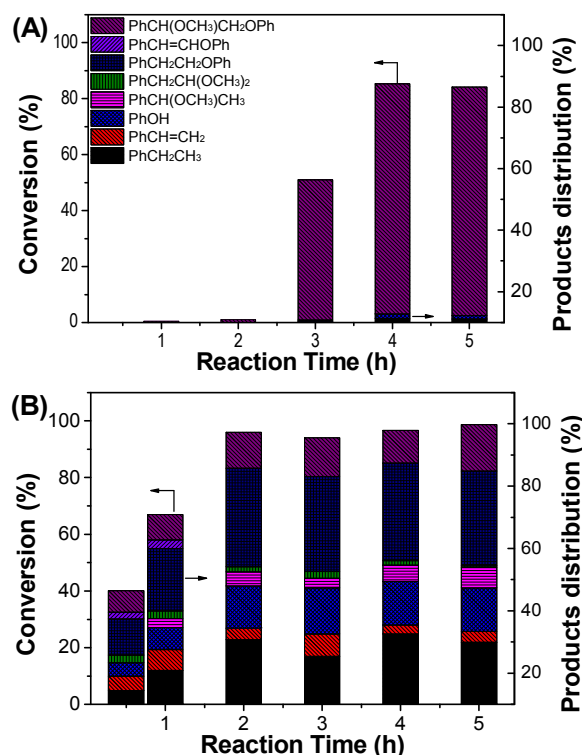


Figure 6. The conversion of the β-O-4-A over the NiS (A) and MoS₂ (B) catalyst. Reaction condition: β-O-4-A 0.2 mmol, catalyst 20 mg, methanol 2.0 mL, H₂ 1.0 MPa, 180 °C. The height of the histogram stands for the conversion.

NiMo sulfide catalyst can obviously restrain the β-O-4-H generation (Figure 2B). Based on the characterization of NiMo sulfide (Figure 5), the introducing Ni species can dilute or separate the surface Mo centers and generate new NiMo cluster¹⁷ with hydrogenation ability. Referring to the catalytic performance of NiS and MoS₂ in the β-O-4-A transformation, the central metal of the redox site could be the Mo, and the hydrogenation site could be the MoS_x or NiMo cluster.

Although the introducing Ni species can restrain the hydrogenolysis of β-O-4-A to β-O-4-H over the NiMo sulfide, the etherification product of β-O-4-E increases. To decrease β-O-4-E, different solvents and introducing metals are screened.

When the non-alcohol solvents such as n-dodecane, 1,4-dioxane, acetonitrile, and N-methyl pyrrolidone were used, low conversions and high ratio of β-O-4-H were obtained (Scheme S8). When ethanol was used as the solvent (Figure S15A), the reaction offered >99% conversion and about 80% products yield with ether bond cleavage in 2 h. When isopropanol was used as solvent (Figure S15B), >99% conversion and 88% products (phenol and ethylbenzene) yield were obtained in 5 h.

For the effect of the solvent on β-O-4-A conversion and β-O-4-H generation, as we proposed in Figure 4, the PhCH·CH₂OPh is a key intermediate, and the high concentration of active hydrogen species on the NiMo sulfide surface should be favorable for the transformation of PhCH·CH₂OPh to β-O-4-H. A competitive adsorption among

solvent, substrate (hydroxyl group of β -O-4-A) and H_2 molecule may exist at the surface of the NiMo sulfide.⁶ N-containing solvent (acetonitrile, and N-methyl pyrrolidone) have strong absorption effect, and their basic hydrolysis products¹⁴ can affect the acid sites of NiMo sulfide, which cause low conversions. When n-dodecane and 1,4-dioxane with lower absorption effect than alcohol are used, H_2 absorption on Mo center can compete with β -O-4-A absorption^{6b} and the concentration of active hydrogen species on the NiMo sulfide surface should be higher, which causes low conversions and high ratio of β -O-4-H. Combined the catalytic ability of NiMo sulfide with competitive adsorption between alcohol and H_2 , the alcohol solvent is a good choice to restrain the generation of β -O-4-H.

For the ratio of β -O-4-E in β -O-4-A conversion products, one tendency exists that the steric hindrance of the alcohol solvent molecular is favorable for reducing the ratio of β -O-4-E (Figure 2B and Figure S15). However, when tertiary butanol is used as the solvent (Figure S15C), the β -O-4-A conversion with C_{β} -OPh cleavage is 18% in 1 h. Butanol contains a tertiary alcohol group with steric bulk and can be used as radical scavenger, which can affect the activation of substrate and H_2 . Furthermore, referring to the concept to reduce the generation of β -O-4-H via competitive adsorption between solvent and H_2 , if β -O-4-A model compound contains a $C_{\gamma}H_2$ -OH structure to compete with solvent alcohol to adsorb on the catalyst, the generation of ether product without C_{β} -OPh cleavage can be restrained. The experiments prove this thought.

When 2-(2-methoxyphenoxy)-1-(4-methoxyphenyl)propane-1,3-diol is used as substrate, the NiMo sulfide can selectively catalyze the cleavage of C_{β} -OPh without aromatic rings hydrogenation, and no hydrogenolysis or etherification product at C_{α} without C_{β} -OPh cleavage is detected (Scheme S9).

Besides solvent screening, we also changed the introducing metal. When Mn, Fe and Co replaced the Ni in the MMo sulfide catalysts, the catalytic performance changed obviously. In the β -O-4-K conversion (Figure S17), when Mn replaced the Ni, the MnMo sulfide catalyst could catalyze the hydrogenation of carbonyl group and ether bond cleavage, and lower β -O-4-K conversions were obtained over FeMo and CoMo sulfide catalysts. In the β -O-4-A conversion (Figure S18), the MMo sulfide catalysts (M=Mn, Fe, Co) offered lower conversion than NiMo sulfide catalyst. Therefore, for the catalysis performance of MMo sulfide catalysts, the promotion of Ni introducing was obvious, which implied the catalytic ability of NiMo cluster in selective cleavage of C_{β} -OPh bond of β -O-4-A.

In the hydrogenation of β -O-4-A, the cooperation between acid-redox sites and hydrogenation sites in NiMo sulfide makes the dehydroxylation-hydrogenation strategy an efficient route, and the advantage of this route makes the catalyst control the main reaction direction. Meanwhile, the structure of the substrate, the competitive adsorption (among substrate, H_2 and solvent), as well as reaction condition (temperature, additives etc.) can regulate the detailed routes, which offer different conversions and products distributions. In this

control-regulate catalysis system, the characterizations of catalyst play a crucial role. Compared with efficient homogeneous catalysts that usually contain single-site catalytic center, heterogeneous catalysts can integrate multiple catalytic centers with different catalytic ability via ingenious preparation process. If these catalytic centers are wisely located in a catalysis micro surrounding, they can provide more possibility. The more possibility are necessary for the lignin transformation. As shown in Figure 5, further work about the optimization of NiMo sulfide catalysts preparation need be done. In addition, study about the accurate structure of catalytic centers will be useful in screening catalysts for lignin conversion.

3. Conclusions

In summary, we present an efficient hydrogenation route for C_{β} -OPh bond cleavage in the β -O-4 lignin model compounds. For 2-phenoxy-1-phenylethanol (β -O-4-A) conversion over the NiMo sulfide catalyst, the efficient reaction route is not via C_{β} -OPh ether bond direct cleavage or C_{α} -OH dehydrogenation to $C_{\alpha}=\text{O}$ before subsequent transformation. The β -O-4-A loses a hydroxy group (C_{α} -OH) at weak and medium strong acid sites of the catalyst. Then the $\text{PhCH}^{\delta+}\text{CH}_2\text{OPh}$ transforms to $\text{PhCH}\cdot\text{CH}_2\text{OPh}$ by obtaining an electron from the catalyst redox cycle. Since the possible intermediate $\text{PhCH}\cdot\text{CH}_2\text{OPh}$ has a much lower C_{β} -OPh bond BDE ($66.9 \text{ kJ}\cdot\text{mol}^{-1}$) than β -O-4-A ($274.0 \text{ kJ}\cdot\text{mol}^{-1}$), the C_{β} -OPh bond breaks easily and generates styrene, ethylbenzene, phenol and various ether products under a hydrogenation condition with alcohol solvent. The cooperation between the acid-redox site and hydrogenation site play a crucial role in this route. Although questions such as etherification product ratio and low catalytic activity still exist during the NiMo sulfide catalyst application, they can be resolved by the concept of competitive adsorption via solvent and substrate structure optimization. Finally, we believe that our finding about the new dehydroxylation-hydrogenation strategy will be useful in screening catalysts for lignin conversion.

Experimental Section

Lignin β -O-4 model compounds synthesis

The β -O-4 lignin model compounds 2-phenoxy-1-phenylethanol (β -O-4-K),^{2b} 2-phenoxy-1-phenylethanol (β -O-4-A),^{2b} 1-(4-methoxyphenyl)-2-phenoxyethanol (β -O-4-K-OCH₃),^{2b} 1-(4-methoxyphenyl)-2-phenoxyethanol (β -O-4-A-OCH₃),^{2b} (2-phenoxyethyl)benzene (β -O-4-H),^{3e} (2-phenoxyvinyl)benzene (β -O-4-O),^{5a} (2-phenoxyethyl)benzene (β -O-4-H),^{3e} (1-methoxy-2-phenoxyethyl)benzene (β -O-4-E)^{7a} and 2-(2-methoxyphenoxy)-1-(4-methoxyphenyl)propane-1,3-diol (model compound with $C_{\gamma}H_2$ -OH structure)^{6a, 18} are synthesized according to the previous procedures. The detailed procedure are provided in Supporting Information.

Catalysts preparation

ARTICLE

Journal Name

The $(\text{NH}_4)_2\text{MoS}_4$ (5.2 g) was dispersed in a nickel chloride solution (200 mL, 20 mmol). After stirring at 100 °C for 6 h, the solid was collected by filtration, washed with distilled water and ethanol, dried at 60 °C under vacuum, followed by calcination in a horizontal furnace at 450 °C for 6 h in an Ar flow (50 mL·min⁻¹) at a 5 °C·min⁻¹ heating rate from 25 °C. The final sample was designated as NiMo sulfide.

The preparation procedures of MMo (M=Mn, Fe, Co) sulfide catalyst were according to the NiMo catalyst, just used $\text{Mn}(\text{OAc})_2$, FeSO_4 and CoCl_2 as the M^{2+} ion precursor. The MoS_2 was obtained by treating the as-prepared $(\text{NH}_4)_2\text{MoS}_4$ in a horizontal furnace at 450 °C for 6 h in an Ar flow. NiS was synthesized according to the previous work.¹⁹

Ether bond dissociation enthalpy

We have calculated the bond dissociation energies (BDE) by employing the Vienna Ab Initio Simulation Package (VASP),²⁰ a periodic plane wave based density functional theory (DFT) program. The BDE value of C–O bonds in different molecular and radical were shown in Table S1.

Procedure for catalytic reactions

In a typical experiment, the substrate (0.2 mmol), catalyst (20 mg), solvent (methanol, 2.0 mL) and a magnetic stirrer were placed into a high-pressured reactor (10 mL). After flushing with Ar for five times, the reactor was charged with 1.0 MPa H_2 and placed into a preheated red copper mantle at the desired temperature. After the reaction, the reactor was quenched to ambient temperature using cooling water. The *n*-dodecane as the standard substance in ethanol solution was added in the reaction mixture, after the filtration with a Teflon filter membrane, the organic products were analyzed by GC-FID (Agilent 7890 A) and GC/MS (GC: Agilent 7890 A, MS: Agilent 5975 C).

Electron Microscopy

The electron microscopy analysis was carried out on the FEI Titan ChemiSTEM at the Ernst Ruska Center Jülich, Germany, equipped with a high angle four quadrant EDX detector and operating at 200kV.

Acknowledgements

This work is supported by the National Natural Science Foundation of China (21422308, 21403216), the Dalian Excellent Youth Foundation (2015J12JH203), and the German Helmholtz Association.

Notes and references

1 (a) J. Zakzeski; P. C. A. Bruijninx; A. L. Jongerius; B. M. Weckhuysen. *Chem. Rev.*, 2010, **110**, 3552-3599; (b) P. Gallezot. *Chem. Soc. Rev.*, 2012, **41**, 1538-1558; (c) C. Xu; R. A. D. Arancón; J. Labidi; R. Luque. *Chem. Soc. Rev.*, 2014, **43**, 7485-7500; (d) P. J. Deuss; K. Barta; J. G. de Vries. *Catal. Sci. Technol.*, 2014, **4**, 1174-1196; (e) T. Prasomsri; M. Shetty; K. Murugappan; Y. Roman-Leshkov. *Energy Environ. Sci.*, 2014, **7**, 2660-2669; (f) X. Chen; N.

Yan. *Catal Surv Asia*, 2014, **18**, 164-176; (g) S. Van den Bosch; W. Schutyser; R. Vanholme; T. Driessen; S. F. Koelewijn; T. Renders; B. De Meester; W. J. J. Huijgen; W. Dehaen; C. M. Courtin; B. Lagrain; W. Boerjan; B. F. Sels. *Energy Environ. Sci.*, 2015, **8**, 1748-1763; (h) R. Ma; K. Cui; L. Yang; X. L. Ma; Y. D. Li. *Chem. Commun.*, 2015, **51**, 10299-10301.

2 (a) C. Li; X. Zhao; A. Wang; G. W. Huber; T. Zhang. *Chem. Rev.*, 2015, **115**, 11559-11624; (b) Z. Strassberger; A. H. Alberts; M. J. Louwerse; S. Tanase; G. Rothenberg. *Green Chem.*, 2013, **15**, 768-774.

3 (a) A. G. Sergeev; J. F. Hartwig. *Science*, 2011, **332**, 439-443; (b) J. Zhang; J. Teo; X. Chen; H. Asakura; T. Tanaka; K. Teramura; N. Yan. *ACS Catal.*, 2014, **4**, 1574-1583; (c) J. Zhang; H. Asakura; J. van Rijn; J. Yang; P. Duchesne; B. Zhang; X. Chen; P. Zhang; M. Saey; N. Yan. *Green Chem.*, 2014, **16**, 2432-2437; (d) H. Konnerth; J. Zhang; D. Ma; M. H. G. Pechtl; N. Yan. *Chem. Eng. Sci.*, 2015, **123**, 155-163; (e) Q. Song; J. Cai; J. Zhang; W. Yu; F. Wang; J. Xu. *Chin. J. Catal.*, 2013, **34**, 651-658; (f) Q. Song; F. Wang; J. Xu. *Chem. Commun.*, 2012, **48**, 7019-7021; (g) K. Barta; G. R. Warner; E. S. Beach; P. T. Anastas. *Green Chem.*, 2014, **16**, 191-196; (h) X. Y. Wang; R. Rinaldi. *ChemSusChem*, 2012, **5**, 1455-1466; (i) V. Molinari; C. Giordano; M. Antonietti; D. Esposito. *J. Am. Chem. Soc.*, 2014, **136**, 1758-1761; (j) P. Kelley; S. Lin; G. Edouard; M. W. Day; T. Agapie. *J. Am. Chem. Soc.*, 2012, **134**, 5480-5483; (k) T. H. Parsell; B. C. Owen; I. Klein; T. M. Jarrell; C. L. Marcum; L. J. Hauptert; L. M. Amundson; H. I. Kenttamaa; F. Ribeiro; J. T. Miller; M. M. Abu-Omar. *Chem. Sci.*, 2013, **4**, 806-813.

4 (a) S. K. Hanson; R. T. Baker. *Acc. Chem. Res.*, 2015, **48**, 2037-2048; (b) B. Sedai; R. T. Baker. *Adv Synth Catal*, 2014, **356**, 3563-3574; (c) S. K. Hanson; R. L. Wu; L. A. Silks. *Angew. Chem. Int. Ed.*, 2012, **51**, 3410-3413; (d) S. Son; F. D. Toste. *Angew. Chem. Int. Ed.*, 2010, **49**, 3791-3794; (e) Y. J. Gao; J. G. Zhang; X. Chen; D. Ma; N. Yan. *ChemPlusChem*, 2014, **79**, 825-834; (f) D. R. Vardon; M. A. Franden; C. W. Johnson; E. M. Karp; M. T. Guarneri; J. G. Linger; M. J. Salm; T. J. Strathmann; G. T. Beckham. *Energy Environ. Sci.*, 2015, **8**, 617-628; (g) J. Zakzeski; A. L. Jongerius; B. M. Weckhuysen. *Green Chem.*, 2010, **12**, 1225-1236.

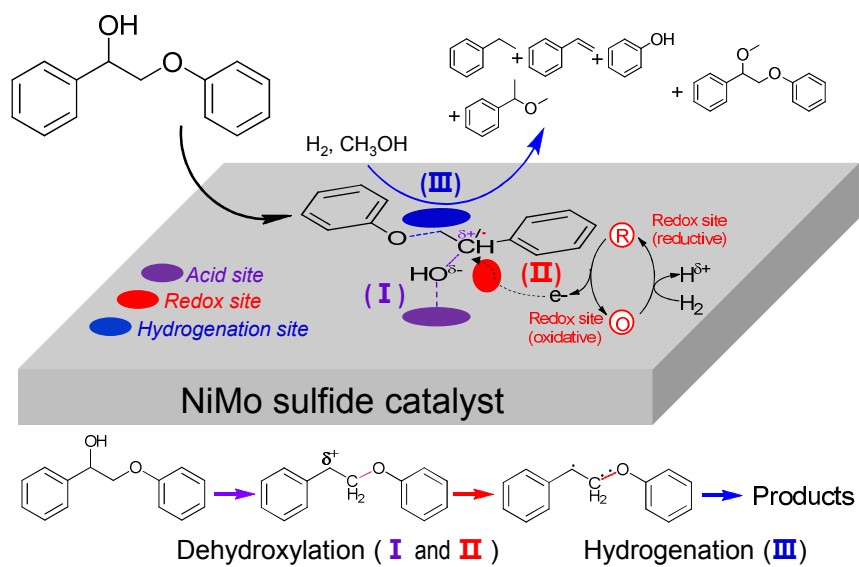
5 (a) M. R. Sturgeon; S. Kim; K. Lawrence; R. S. Paton; S. C. Chmely; M. Nimlos; T. D. Foust; G. T. Beckham. *ACS Sustainable Chem. Eng.*, 2014, **2**, 472-485; (b) P. J. Deuss; M. Scott; F. Tran; N. J. Westwood; J. G. de Vries; K. Barta. *J. Am. Chem. Soc.*, 2015, **137**, 7456-7467; (c) S. Y. Jia; B. J. Cox; X. W. Guo; Z. C. Zhang; J. G. Ekerdt. *ChemSusChem*, 2010, **3**, 1078-1084; (d) J. Hu; D. K. Shen; S. L. Wu; H. Y. Zhang; R. Xiao. *RSC Adv.*, 2015, **5**, 43972-43977; (e) L. Yang; Y. D. Li; P. E. Savage. *Ind. Eng. Chem. Res.*, 2014, **53**, 2633-2639.

6 (a) Q. Song; F. Wang; J. Cai; Y. Wang; J. Zhang; W. Yu; J. Xu. *Energy Environ. Sci.*, 2013, **6**, 994-1007; (b) R. Ma; W. Hao; X. Ma; Y. Tian; Y. Li. *Angew. Chem. Int. Ed.*, 2014, **53**, 7310-7315.

7 (a) J. M. Nichols; L. M. Bishop; R. G. Bergman; J. A. Ellman. *J. Am. Chem. Soc.*, 2010, **132**, 12554-12555; (b) S. C. Chmely; S. Kim; P. N. Ciesielski; G. Jimenez-Oses; R. S. Paton; G. T. Beckham. *ACS Catal.*, 2013, **3**, 963-974; (c) X. Zhou; J. Mitra; T. B. Rauchfuss. *ChemSusChem*, 2014, **7**, 1623-1626; (d) T. vom Stein; T. den Hartog; J. Buendia; S. Stoychev; J. Mottweiler; C. Bolm; J. Klankermayer; W. Leitner. *Angew. Chem. Int. Ed.*, 2015, **54**, 5859-5863; (e) M. C. Haibach; N. Lease; A. S. Goldman. *Angew. Chem. Int. Ed.*, 2014, **53**, 10160-10163; (f) R. G. Harms; Markovits, II; M. Drees; H. C. Herrmann; M. Cokoja; F. E. Kuhn. *ChemSusChem*, 2014, **7**, 429-34.

- 8 (a) A. C. Atesin; N. A. Ray; P. C. Stair; T. J. Marks. *J. Am. Chem. Soc.*, 2012, **134**, 14682-14685; (b) Z. Li; R. S. Assary; A. C. Atesin; L. A. Curtiss; T. J. Marks. *J. Am. Chem. Soc.*, 2013, **136**, 104-107; (c) J. D. Nguyen; B. S. Matsuura; C. R. Stephenson. *J. Am. Chem. Soc.*, 2014, **136**, 1218-1221; (d) A. Rahimi; A. Ulbrich; J. J. Coon; S. S. Stahl. *Nature*, 2014, **515**, 249-252; (e) C. S. Lancefield; O. S. Ojo; F. Tran; N. J. Westwood. *Angew. Chem. Int. Ed.*, 2015, **54**, 258-262.
- 9 R. Parthasarathi; R. A. Romero; A. Redondo; S. Gnanakaran. *J. Phys. Chem. Lett.*, 2011, **2**, 2660-2666.
- 10 J. L. Wen; T. Q. Yuan; S. L. Sun; F. Xu; R. C. Sun. *Green Chem.*, 2014, **16**, 181-190.
- 11 (a) J. He; C. Zhao; J. A. Lercher. *J. Am. Chem. Soc.*, 2012, **134**, 20768-20775; (b) D. J. Rensel; S. Rouvimov; M. E. Gin; J. C. Hicks. *J. Catal.*, 2013, **305**, 256-263; (c) M. R. Sturgeon; M. H. O'Brien; P. N. Ciesielski; R. Katahira; J. S. Kruger; S. C. Chmely; J. Hamlin; K. Lawrence; G. B. Hunsinger; T. D. Foust; R. M. Baldwin; M. J. Bidy; G. T. Beckham. *Green Chem.*, 2014, **16**, 824-835; (d) J. A. Onwudili; P. T. Williams. *Green Chem.*, 2014, **16**, 4740-4748; (e) C. Z. Li; M. Y. Zheng; A. Q. Wang; T. Zhang. *Energy Environ. Sci.*, 2012, **5**, 6383-6390; (f) C. Zhao; J. A. Lercher. *ChemCatChem*, 2012, **4**, 64-68; (g) M. Zaheer; J. Hermannsdorfer; W. P. Kretschmer; G. Motz; R. Kempe. *ChemCatChem*, 2014, **6**, 91-95; (h) M. V. Galkin; S. Sawadjoon; V. Rohde; M. Dawange; J. S. M. Samec. *ChemCatChem*, 2014, **6**, 179-184; (i) S. K. Singh; J. D. Ekhe. *Catal. Sci. Technol.*, 2015, **5**, 2117-2124; (j) K. Barta; T. D. Matson; M. L. Fettig; S. L. Scott; A. V. Iretskii; P. C. Ford. *Green Chem.*, 2010, **12**, 1640-1647; (k) C. R. Kumar; N. Anand; A. Kloekhorst; C. Cannilla; G. Bonura; F. Frusteri; K. Barta; H. J. Heeres. *Green Chem.*, 2015, **17**, 4921-4930; (l) A. Narani; R. K. Chowdari; C. Cannilla; G. Bonura; F. Frusteri; H. J. Heeres; K. Barta. *Green Chem.*, 2015, **17**, 5046-5057.
- 12 (a) B. Sawatlon; T. Wititsuwannakul; Y. Tantirungrotechai; P. Surawatanawong. *Dalton Trans.*, 2014, **43**, 18123-18133; (b) D. Weickmann; B. Plietker. *ChemCatChem*, 2013, **5**, 2170-2173.
- 13 (a) J. Löfstedt; C. Dahlstrand; A. Orebom; G. Meuzelaar; S. Sawadjoon; M. V. Galkin; P. Agback; M. Wimby; E. Corresa; Y. Mathieu; L. Sauvanud; S. Eriksson; A. Corma; J. S. M. Samec. *ChemSusChem*, 2016, **9**, 1392-1396; (b) V. M. L. Whiffen; K. J. Smith. *Energy Fuel*, 2010, **24**, 4728-4737; (c) A. L. Jongerius; R. Jastrzebski; P. C. A. Bruijninx; B. M. Weckhuysen. *J. Catal.*, 2012, **285**, 315-323; (d) W. S. Lee; Z. S. Wang; R. J. Wu; A. Bhan. *J. Catal.*, 2014, **319**, 44-53.
- 14 H. L. Fan; Y. Y. Yang; J. L. Song; Q. L. Meng; T. Jiang; G. Y. Yang; B. X. Han. *Green Chem.*, 2015, **17**, 4452-4458.
- 15 B. Zhang; C. Li; T. Dai; G. W. Huber; A. Wang; T. Zhang. *RSC Adv.*, 2015, **5**, 84967-84973.
- 16 P. M. Mortensen; J. D. Grunwaldt; P. A. Jensen; K. G. Knudsen; A. D. Jensen. *Appl. Catal., A*, 2011, **407**, 1-19.
- 17 A. Cho; J. J. Lee; J. H. Koh; A. Wang; S. H. Moon. *Green Chem.*, 2007, **9**, 620-625.
- 18 J. Zhang; Y. Liu; S. Chiba; T.-P. Loh. *Chem. Commun.*, 2013, **49**, 11439-11441.
- 19 L. L. Wang; Y. C. Zhu; H. B. Li; Q. W. Li; Y. T. Qian. *J. Solid State Chem.*, 2010, **183**, 223-227.
- 20 (a) G. Kresse; J. Furthmuller. *Comp. Mater. Sci.*, 1996, **6**, 15-50; (b) G. Kresse; J. Hafner. *Phys. Rev. B*, 1993, **47**, 558-561.

Graphical abstract:



Herein, different from reported strategies beginning with dehydrogenation, we present an efficient dehydroxylation-hydrogenation strategy in the lignin β -O-4 model compounds transformation over a NiMo sulfide catalyst.